University of Texas Rio Grande Valley
ScholarWorks @ UTRGV

Theses and Dissertations

8-2022

# Thermal Convection in a Cylindrical Annulus Filled with Porous Material

Anirban Ray
*The University of Texas Rio Grande Valley*

Follow this and additional works at: https://scholarworks.utrgv.edu/etd

 Part of the Mathematics Commons

## Recommended Citation

Ray, Anirban, "Thermal Convection in a Cylindrical Annulus Filled with Porous Material" (2022). *Theses and Dissertations*. 1083.
https://scholarworks.utrgv.edu/etd/1083

This Thesis is brought to you for free and open access by ScholarWorks @ UTRGV. It has been accepted for inclusion in Theses and Dissertations by an authorized administrator of ScholarWorks @ UTRGV. For more information, please contact justin.white@utrgv.edu, william.flores01@utrgv.edu.

# THERMAL CONVECTION IN A CYLINDRICAL ANNULUS FILLED WITH POROUS MATERIAL

A Thesis

by

ANIRBAN RAY

Submitted in partial fulfillment of the

requirements for the degree of

MASTER OF SCIENCE

Major Subject: Mathematics

The University of Texas Rio Grande Valley

August 2022

# THERMAL CONVECTION IN A CYLINDRICAL ANNULUS FILLED WITH POROUS MATERIAL

A Thesis
by
ANIRBAN RAY

COMMITTEE MEMBERS

Dr. Dambaru Bhatta
Chair of Committee

Dr. Andras Balogh
Committee Member

Dr. Paul Bracken
Committee Member

Dr. Zhijun Qiao
Committee Member

August 2022

Copyright 2022 Anirban Ray
All Rights Reserved

ABSTRACT

Ray, Anirban, Thermal convection in a cylindrical annulus filled with porous material. Master of Science (MS), August, 2022, 41 pp., 5 tables, 23 figures, references, 31 titles.

Here a study on thermal convection in a porous vertical cylindrical annulus which is heated from below is carried out. The walls are considered to be impermeable that is the velocity is 0 at the boundary walls. The cylindrical annulus is radially insulated .The governing system consists of the continuity equation, Darcy-Boussinesq equation, heat equation and the equation of state. Employing weakly non-linear approach, the basic state system and the perturbed system are derived. After obtaining the solutions to the basic state system, the pressure term in perturbed system is eliminated by taking double curl, and then eliminating the velocity, a partial differential equation in the linearized perturbed temperature is obtained. This partial differential equation is solved in terms of Bessel and trigonometric functions using separation of variables method. For axisymmetric case, the solution contains the zeroth order Bessel functions of the first and second kind. Computational results for the temperature are presented in tabular and graphical forms.

# DEDICATION

This thesis is dedicated to my family and to my late father. They have supported me throughout my education and in pursuing my dreams.

ACKNOWLEDGMENTS

I express my gratitude towards the thesis committee members especially the committee chair, Dr. Dambaru Bhatta. I thank him for his patience and support as well as for motivating me to never give up. I express my sincere thanks to Dr. Zhijun Qiao, Dr. Andras Balogh and Dr. Paul bracken for serving as committee member in my thesis. Also Dr. Qiao and Dr. Bhatta deserve special thanks for guiding me in my PGRA project. I am thankful to Dr. Mahanthesh Basavarajappa for his help during preparation of this thesis. I would like to thank my family for motivating me as well. Lastly, I thank my friends especially Zhenteng Zeng for helping me during these semesters. I would also like to thank the Maths department at UTRGV for providing me with all the assistance and support needed to succeed in completing my degree efficiently.

TABLE OF CONTENTS

Page

LIST OF TABLES

Page

LIST OF FIGURES

Page

# CHAPTER I

## INTRODUCTION

A porous medium or a porous material is a material containing pores or voids. It is a material consisting of a solid matrix with interconnected voids. The solid matrix is rigid in usual situation, but it may undergo small deformation. The interconnectedness of the void (the pores) allows the flow of one or more fluids through the material. In the simplest scenario, the void is saturated by a single fluid which is called single phase flow. In two-phase flow a liquid and a gas share the void space. The interconnectedness of the void (the pores) allows the flow of one or more fluids through the material. In the simplest situation ("single-phase flow") the void is saturated by a single fluid. In "two-phase flow" a liquid and a gas share the void space .

In natural porous media the distribution of pores with respect to shape and size is irregular.Examples of natural porous media are beach sand, sandstone, limestone, rye bread, wood, human tissue. On the pore scale(the microscopic scale) the flow quantities of interest are measured over areas that cross many pores, and such space averaged(macroscopic) quantities change in regular manner with respect to space and time, and hence are applicable to theoretical treatment. The usual way of deriving the laws governing the macroscopic variables is to begin with the standard equation obeyed by the fluid and to obtain macroscopic equations by averaging over volumes or areas containing any pores.In this approach a macroscopic variable is defined as an appropriate mean over a representative elementary volume(r.e.v); this operation yields the value of that variable at the centroid of the r.e.v. It is assumed that the result is independent of the size of

the representative elementary volume. The length scale of the r. e. v. is much bigger that the pore scale, but comparatively smaller that the length scale of the macroscopic flow domain.

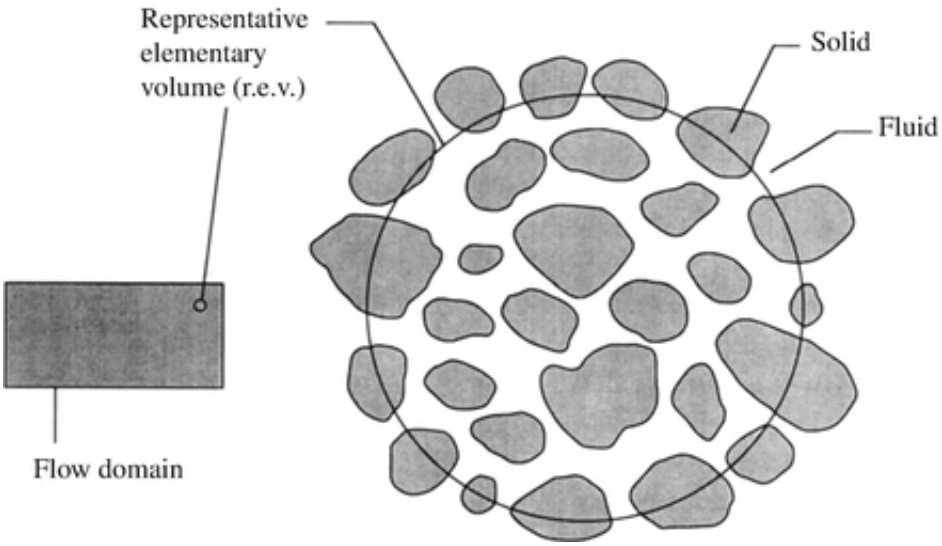


Figure 1: The representative elementary volume (r.e.v.): the figure illustrates the intermediate size relative to the sizes of the flow domain and the pores.

The representative elementary volume serves the purpose of macroscopic study of a porous media. In general a porous media has microscopic pores and innumerable in a given area of space. The idea of r.e.v is used to study a certain section of the porous media where the pores are visible and numerically comprehensible to a certain extent.

Porosity: A porous medium is most often characterized by its porosity. The porosity $\phi$ of a porous medium is defined as a fraction of the total volume of the medium that is occupied by the void space. Thus $1-\phi$ is the fraction that is occupied by solid. In defining $\phi$ in this way we are assuming that all the void space is connected. If one has to deal with a medium in which some of the pore space is disconnected from the remainder, then one has to introduce an effective porosity defined as the ratio of connected void to the total volume. Effective porosity is concerned with the pore space accessible to the flow.

Permeability: The permeability of a porous medium is a measure of the ease with which a fluid will flow through the medium; the higher the permeability, the higher the flow rate for a given hydraulic gradient. The permeability is a statistical average of the fluid conductivities of the all the flow channels in the solid body. Permeability is a property of the porous medium that measures the capacity and ability of the formation to transit fluids. Foolowing is a table on properties of some common porous media based on data compiled by Scheidegger (1974) and Bejan and Lage (1991

Table 1: Properties of common porous materials

| Material | Porosity $\varphi$ | Permeability $K$[cm2] | Surface per unit volume [cm−1] |
|---|---|---|---|
| Agar Agra | | 2 × 10−10–4.4 × 10−9 | |
| Brick | 0.12–0.34 | 4.8 × 10−11–2.2 × 10−9 | |
| Cigarette | | 1.1 × 10−5 | |
| Coal | 0.02–0.12 | | |
| Leather | 0.56–0.59 | 9.5 × 10−10–1.2 × 10−9 | 1.2 × 104–1.6 × 104 |
| Sand | 0.37–0.50 | 2 × 10−7–1.8 × 10−6 | 150–220 |
| Soil | 0.43–0.54 | 2.9 × 10−9–1.4 × 10−7 | |
| Fibre Glass | 0.88–0.93 | | 560–770 |
| Hair | 0.95–0.99 | | |
| Black slate powder | 0.57–0.66 | 4.9 × 10−10–1.2 × 10−9 | 7 × 103–8.9 × 103 |

A porous medium or a porous material is a material containing pores(voids). The pores are typically filled with a fluid(fluid or gas); Convective heat and mass transport in porous media has a wide range of applications:

- Filtering Technology: Water Purification, Kidney/Renal filtration(removes waste from blood), Sewage treatment;
- Casting, Molding, Solidification(Crystal growth), Mushy layer;
- Reservoirs: Water movements in geothermal reservoirs, Enhanced recovery of petroleum

reservoirs, Aquifers;

- Heat Pipes, Heat exchangers,Thermal insulation, Coal combustor, Nuclear waste reposito-ries;
- Biomedical applications: Tissue engineering, Porous materials for drug delivery, Orthopedics implants(providing biological fixation, scaffolds for tissue, ceramics for bone reconstruction), Blood flow through aorta (aortic wall treated of porous layer);
- Underground spreading for chemical waste, Prevention of Coastal erosion, snow, Fuel cells, carbon paper, catalytic reactors, Grain storage, Foams etc.

Some examples used in real life are mentioned below:


Figure 2: Heat exchanger

Porous Aluminum is very useful for heat transfer. In general Aluminum is for heat transfer due to its high thermal conductivity and porous Aluminum is more efficient due to its high internal surface area compared to its volume. The thermal conductivity of the porous aluminium has been

tested by Technical University of Freiberg though the thermal conductivity depends on the pore size. The thermal conductivity lies in the range 30 – 50 W/(m*K). Thus porous aluminium is very well suited for heat transfer purposes. Due to high volume porosity it is also very useful in convective heat transfer as it absorbs heat due to its large internal surface as transfers it to solid boby or fluid.

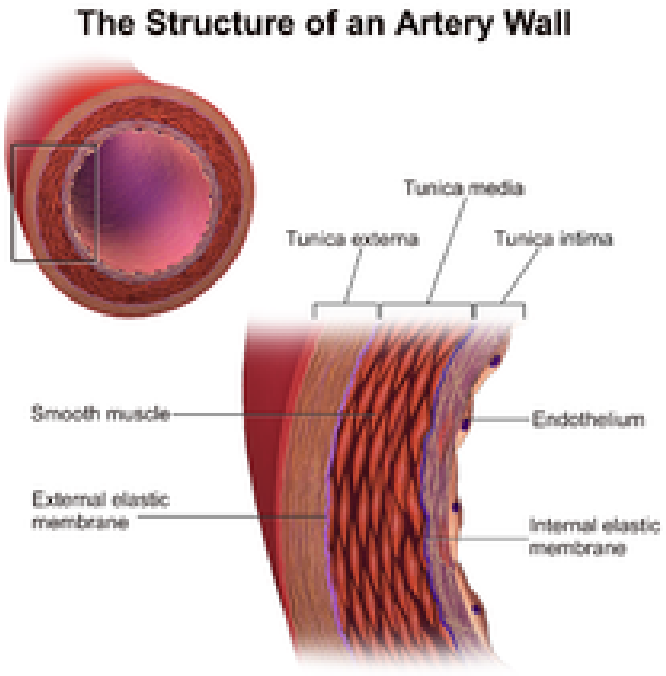


Figure 3: Artery walls

The walls of Artery are porous with very fine-pores and mostly made of muscle.The blood flow through arteries is Non-Newtonian wich means the flow does not obey Newton's law of viscosity. Blood flow through arteries is urbulent in nature but under high conditions the blood flow becomes laminar. Blood flow through arteries is acase of non-newtonian flow through a porous media. Artery walls have varying porosities in different regions. A detailed study of Newtonian blood flow through an artery has been carried out by K. R amakrishnan(2019). There he studied three cases. (i) Porous material in the upper wall have more permeability than in the lower wall (ii)

Porous material in the upper and lower walls have the same permeability and (iii) Porous material in the lower wall have more permeability than in the upper wall.

Petroleum Reservoir

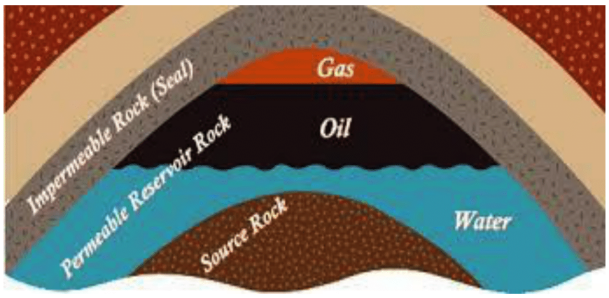


roxannaoil.com/2016/11/source-rock-as-a-reservoir/

Aquifer

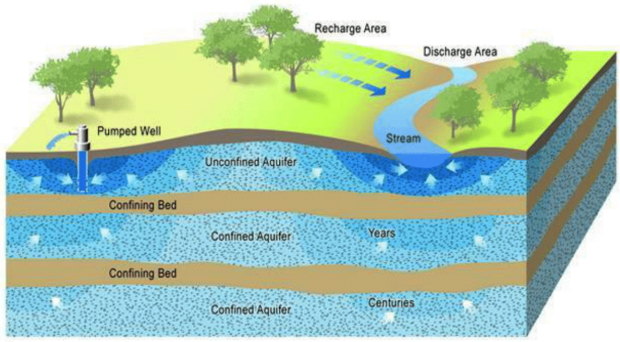


www.dtn.com/wp-content/uploads/2016/05/aquifer_diagram_crop.jpg.webp

Figure 4: Aquifer

Petroleum reservoir and aquifer are other porous media examples.

Though transfer through a porous media is generally done at macrscopic level every analysis begins with study at microscopic level. Through nanaoparticel tracking the discrepancy between theoretical and experimental accuracy can be bridged to cerrtain extent. Detailed analysis of nanoparticle tracking in porous media has been done by Daniel K. Schwartz and Charles M.

Knobler(2020)

Darcy's Law: Henry Darcy's (1856) investigations into the hydrology of the water supply of Dijon and his experiments on steady-state unidirectional flow in a uniform medium revealed a proportionality between flow rate and the applied pressure difference. In modern notation this is expressed, in refined form, by

$$v = -\frac{K}{\mu}\frac{\partial P}{\partial x} \tag{1}$$

Here represents $\frac{\partial P}{\partial x}$ is the pressure gradient in the flow direction and $\mu$ represents the dynamic viscosity of the fluid. The coefficient K is independent of the nature of the fluid but it depends on the geometry of the medium. It has dimensions (length)$^2$ and is called the specific permeability or intrinsic permeability of the medium. It should be noted that in 1 . One needs to take averages over the fluid phase before introducing a Darcy drag term.In three dimensions, 1 generalizes

$$\nabla P = -\frac{\mu}{K}\overrightarrow{u} \tag{2}$$

where now the permeability K is in general a second-order tensor. For the case of an isotropic medium the permeability is a scalar and 2 simplifies to

$$v = -\frac{K}{\mu}\frac{\partial P}{\partial x}$$

Values of K for natural materials vary widely. Typical values for soils, in terms of the unit m$^2$, are: clean gravel $10^{-7}$–$10^{-9}$, stratified clay $10^{-13}$–$10^{-16}$, and unweathered clay $10^{-16}$–$10^{-20}$. Workers concerned with geophysics often use as a unit of permeability the Darcy, which equals $0.987 \times 10^{12}$ m$^2$. Darcy's law has been verified by the results of many experiments. Theoretical

backing for it has been obtained in various ways, with the aid of either deterministic or statistical models. It is interesting that Darcy's original data may have been affected by the variation of viscosity with temperature.If $K$ is dependent on geometrical factors of the medium then $K$ can be calculated for at least simple cases of geometry. A lot of work has been done on this which has been well compiled by Dullien(1992).

Many authors have used statistical concepts in the theoretical support for Darcy's law. This theoretical work is not restricted to only homogeneous structures but also non-homogeneous structures however it is assumed that there are no sudden changes to the structure. If the medium has periodic structure, then the homogenization method can be used to obtain mathematically rigorous results. The method is explained in detail by Ene and Polisˇevski (1987), Mei et al. (1996), and Ene (2004). The first authors to derive Darcy's law without assuming incompressibility, and they go on to prove that the permeability is a symmetric positive-definite tensor. For Newtonian fluids, the momentum and mass conservation are quantitatively expressed by the Navier-Stokes equations. Sometimes they come with a state equation linking pressure, temperature, and density. They result from applying Isaac Newton's second law to fluid motion and from the premise that pressure and diffusing viscous terms which together describe viscous flow are added to the fluid's stress. The Navier-Stokes equations differ from the closely related Euler equations in that they simulate viscous flow as well as viscosity, whereas the Euler equations solely model inviscid flow. Since the Navier-Stokes is a parabolic equation as a result, it has greater analytical properties but less mathematical structure. The equation is given by

$$\frac{\partial \overrightarrow{u}}{\partial t} + \left(\overrightarrow{u} \cdot \nabla\right)\overrightarrow{u} - \nu\frac{\mu}{\rho_0}\nabla^2\overrightarrow{u} = -\nabla\left(\frac{P}{\rho_0}\right) + \overrightarrow{g}$$

where $\nu = \frac{\mu}{\rho_0}$

Brinkman Equation:: An aternative version to Darcy's law is Brinkman's equation. In this equation the inertial

term are removed. The equation is

$$\nabla P = -\frac{\mu}{K}\overrightarrow{u} + \hat{\mu}\nabla^2\overrightarrow{u}$$

where $\hat{\mu}$ is the effective viscosity. This equation is modelled in analogy with the Navier-Stokes equation. Now the equation has two terms for viscosity.

Wooding(1957) and many others working on convection in porous media extended equation (2) to involve a convective difference term.

$$\rho_f \left[\frac{\partial \overrightarrow{V}}{\partial t} + \left(\overrightarrow{V}\cdot\nabla\right)\overrightarrow{V}\right] = -\nabla P - \frac{\mu}{K}\overrightarrow{v}$$

This equation was obtained in analogy with with Navier-Stokes Equation.

Non-Newtonian and Newtonian fluids:

A Newtonian fluid is one in which satisfies Newton's law of viscosity. The local strain rate is linearly dependent on the viscous stresses resulting from its flow at every place. The rate at which the fluid's velocity vector changes determines how much stress is there.

Only when the tensors describing the viscous stress and strain rate are coupled by a constant viscosity tensor that is independent of the stress state and flow velocity can a fluid be said to be Newtonian. The viscosity tensor is reduced to two real coefficients, which describe the fluid's resistance to continuous shear deformation and continuous compression or expansion, respectively, if the fluid is also isotropic (mechanical properties are the same in any direction).Water, air, alcohol, glycerol, and thin motor oil are all examples of Newtonian fluids.

A Non-Newtonian fluid does not obey Newton's law of viscosity that the rate of change of local strain is not linearly dependent on the shear stress tensor. Some examples of Non-Newtonian fluids are Soap solutions, cosmetics, and toothpaste Food such as butter, cheese, jam, mayonnaise, soup, taffy, and yogurt Natural substances such as magma, lava, gums, honey, and extracts such as vanilla extract Biological fluids such as blood, saliva, semen, mucus, and synovial fluid Slurries

such as cement slurry and paper pulp, emulsions such as mayonnaise, and some kinds of dispersions.

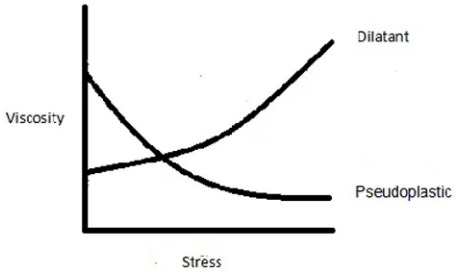


Figure 5: This chart shows how viscosity changes with respect to the amount of shear or stress applied to the fluid.

The principle problem in heat transfer engineering is to determine the relationship between the heat transfer rate and the driving temperature difference. In nature, many saturated porous media interact thermally with one another and with solid surfaces that confine them or are embedded in them. Here we analyze the basic heat transfer question by looking only at forced convection situations, in which the fluid flow is caused (forced) by an external agent unrelated to the heating effect. Some fundamental aspects of the subject have been discussed by Lage and Narasimhan (2000) and the topic has been reviewed by Lauriat and Ghafir (2000).Forced convection in cylinder has been worked by Kimura (1988).

Rayleigh's Number: Rayleigh's number is a dimensionless number in fluid dynamics that characterizes the flow-regime of the flow. In a certain range of this number the flow is turbulent and in a certain lower range the flow is laminar and under a even lower value there is no fluid flow and heat transfer takes place by conduction instead of convection. Rayleigh number in flow in a porous media is also known as Rayleigh-Darcy number and is given by the expression

$$R_a = \frac{\rho_0 g \beta \triangle T K h (\rho c_P)_f}{\mu \kappa_m}$$

Rayleigh number is named after the prominent late physicist Lord Rayleigh. He made a lot of contributions to other fields of Physics as well. Some of his his contributions include Rayleigh's scattering and formulating the mathematics of Taylor-coulette flow. Another important quantity that appears in study of convective heat transfer is called Nusselt number denoted as $Nu$. It is also dimmensionless number closely related to the Rayleigh's number. It is defined as the ratio of convective heat transfer to the conductive heat transfer at the boundary of the fluid. A zero Nusselt number represents a purely conductive heat transfer, a low range of Nusselt number between 0 to 10 represents a laminar flow whereas a large range of typically between 10 to 100 represents a turbulent flow. It was named after the physicist Wilhelm Nusselt. A detailed comparison of Nusselt number against Rayleigh's number was done by Yasuyuki Iwase and Satoru Honda(1996) for a spherical shell. following is a graph showing a comparison between $R_a$ and $Nu$ in a spherical shell.

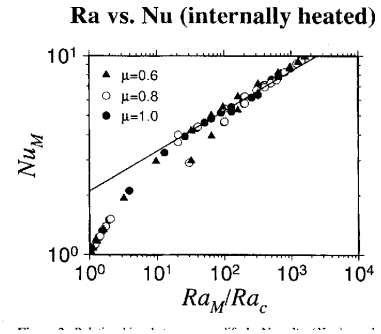


Figure 6: Relationship between Nusselt (Nu) and Rayleigh (Ra) numbers for the 3-D spherical shell convection

# CHAPTER II

## MATHEMATICAL FORMULATION

In this section, we mathematically formulate the problem and introduce the necessary equations and set the background for the solution.

Our problem is to analyze thermal convection in a porous vertical cylindrical annulus of height $h$ with inner radius $R_i$ and outer radius $R_o$. The annulus is heated from below and curved surfaces are insulated and all the sides are impermeable. We introduce the governing equations which are continuity equation, Darcy-Boussinesq equation and the heat equation that govern the heat flow filled with the porous medium. The cylindrical coordinates $(r, \phi, z)$ is presented in figure below.

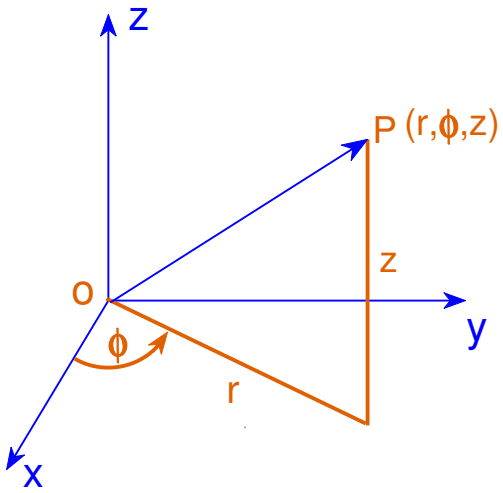


Figure 7: Cylindrical co-ordinate system

The geometry of the problem we are dealing with is shown below.

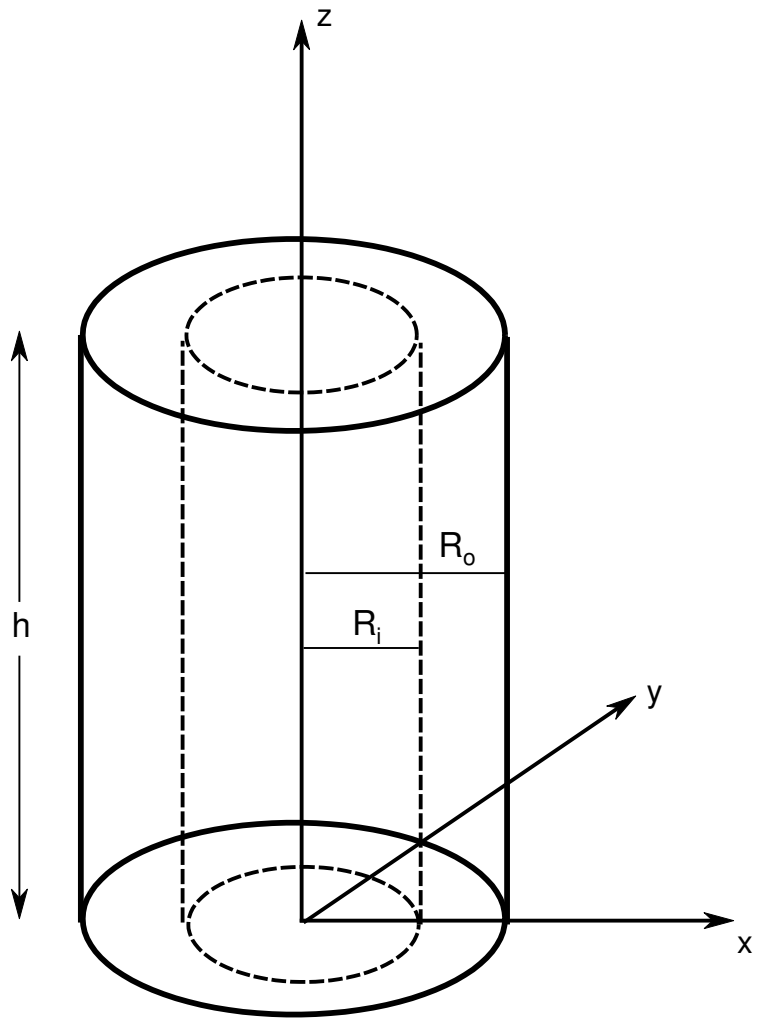


Figure 8: Geometrical sketch of the problem

This the geometrical representation of the problem at hand. The solid cylinder represents the outer cylinder of radius $R_0$ and the dotted line represents the inner cylinder of radius $R_i$. The region between the two cylinders is filled with a porous media.

Governing system consists of the following equations:

$$Continuity \quad Equation \qquad \nabla \cdot \overrightarrow{u} = 0 \tag{3}$$

$$Darcy - Boussinesq \quad Equation \qquad \nabla P = -\frac{\mu}{K}\overrightarrow{u} + \rho_f \overrightarrow{g} \tag{4}$$

$$Temperature \quad Equation \qquad (\rho c_P)_f \overrightarrow{u} \cdot \nabla T = \kappa_m \nabla^2 T \tag{5}$$

$$State \quad Equation \qquad \rho_f = \rho_0 \{1 - \beta (T - T_0)\} \tag{6}$$

where $\overrightarrow{u}, P$ and $T$ represent the velocity, pressure and temperature, respectively. Here $c_P$ denotes the specific heat at a constant pressure, $\beta$ represents thermal expansion coefficient, $\mu$ represents the dynamic viscosity of the fluid, $K$ denotes permeability, $\overrightarrow{g}$ is acceleration due to gravity. Also, $\rho_f$ is the density of the fluid phase and $\kappa_m = \varphi\kappa_f + (1-\varphi)\kappa_s$ where $\kappa_m$ denotes the thermal conductivity of the melt, $\kappa_s, \kappa_f$ denote the thermal conductivity of the solid part and the fluid part, respectively. $\varphi$ represents the porosity. $T_0$ and $\rho_0$ denote the reference temperature and reference density, respectively.

Boundary conditions are

$$T = T_0 \quad at \quad z = h \tag{7}$$

$$T = T_0 + \triangle T \quad at \quad z = 0 \tag{8}$$

$$\frac{\partial T}{\partial r} = 0 \quad at \quad r = R_0, R_i \tag{9}$$

$$u_z = 0 \quad at \quad z = 0, h \tag{10}$$

$$u_r = 0 \quad at \quad r = R_0, R_i \tag{11}$$

where $\overrightarrow{u} =< u_r, u_\phi, u_z >$.

Nondimensionalization of the system is done in the following steps

To nondimensionalize, we use the following:

$$\hat{T} = \frac{T - T_0}{\triangle T}$$
$$\hat{r} = \frac{r}{h}, \quad \hat{z} = \frac{z}{h}$$
$$\hat{\overrightarrow{u}} = \frac{\overrightarrow{u}\,(\rho c_P)_f}{\kappa_m}$$
$$\hat{P} = (P - P_0 + \rho_0 g z)\,\frac{K\,(\rho c_P)_f}{\mu \kappa_m}$$

The corresponding governing equations (3),(4),(5),(6) the nondimmensionalised form is obtained as

$$\nabla \cdot \hat{\overrightarrow{u}} = 0$$
$$\nabla \hat{P} + \hat{\overrightarrow{u}} - R_a \hat{T}\,\hat{k} = 0$$
$$\hat{\overrightarrow{u}} \cdot \nabla \hat{T} = \nabla^2 \hat{T}$$

where $R_a = \frac{\rho_0 g \beta (\triangle T) K h (\rho c_P)_f}{\mu \kappa_m}$ is the Rayleigh number.

Dropping the hats, the system becomes

$$\nabla \cdot \overrightarrow{u} = 0 \tag{12}$$
$$\nabla P + \overrightarrow{u} - R_a T\,\hat{k} = 0 \tag{13}$$
$$\overrightarrow{u} \cdot \nabla T = \nabla^2 T \tag{14}$$

The boundary conditions (7), (8) are transformed as

$$T = 0 \quad at \quad z = 1 \tag{15}$$
$$T = 1 \quad at \quad z = 0 \tag{16}$$

Now, we use weakly non linear approach to seperate the basic state and the perturbed state systems. Separating the original variables into basic state (no flow) and perturbed state, we can express

$$\overrightarrow{u}(r,\phi,z) = \overrightarrow{U} + \epsilon\overrightarrow{q}(r,\phi,z) \tag{17}$$

$$P(r,\phi,z) = P_b(z) + \epsilon P(r,\phi,z) \tag{18}$$

$$T(r,\phi,z) = T_b(z) + \epsilon\theta(r,\phi,z) \tag{19}$$

where $\overrightarrow{U}, P_b(z), T_b(z)$ are basic state variables, $\overrightarrow{q}, P(r,\phi,z), \theta(r,\phi,z)$ are the perturbation variables and $\epsilon$ is a small parmeter.

Using equations (30), (18), (19) in equations (12), (13), (14) and (6), we get

$$\nabla\cdot\left(\overrightarrow{U} + \epsilon\overrightarrow{q}\right) = 0 \tag{20}$$

$$\nabla(P_b + \epsilon P) + \left(\overrightarrow{U} + \overrightarrow{\epsilon q}\right) - R_a(T_b(z) + \epsilon\theta(r,\phi,z))\hat{k} = \overrightarrow{0}.$$

$$\left(\overrightarrow{U} + \epsilon\overrightarrow{q}\right)\cdot\nabla(T_b(z) + \epsilon\theta(r,\phi,z)) = \nabla^2(T_b(z) + \epsilon\theta(r,\phi,z))$$

$$\rho_f = \rho_0(1 - \beta(T_b(z) + \epsilon\theta(r,\phi,z) - T_0)) \tag{21}$$

Separating the terms with $\epsilon$ and without $\epsilon$ we obtain the basic state and the perturbed state systems respectively.

The basic state system equations are given as follows:

As the basic state has no flow, we have

$$\overrightarrow{U} = \overrightarrow{0} \tag{22}$$

$$\nabla(P_b) - R_a T_b\hat{k} = 0 \tag{23}$$

$$\nabla^2(T_b(z)) = 0 \tag{24}$$

The solutions to the basic state equations (22), (23), (24) are

$$\overrightarrow{U} = \overrightarrow{0}$$
$$T_b = 1 - z$$
$$P_b(z) = R_a\left(z - \frac{z^2}{2}\right)$$

The perturbed system equations are given below:

$$\nabla \cdot \overrightarrow{q} = 0 \tag{25}$$

$$\nabla P + \overrightarrow{q} - R_a \theta \hat{k} = 0 \tag{26}$$

$$\overrightarrow{q} \cdot \nabla T_b + \overrightarrow{q} \cdot \nabla \theta = \nabla^2 \theta \tag{27}$$

# CHAPTER III

## SOLUTION PROCEDURE

Here we present the solution procedure to obtain the temperature variable for the following perturbed system

$$\nabla \cdot \vec{q} = 0 \tag{28}$$

$$\nabla P + \vec{q} - R_a \theta \hat{k} = 0 \tag{29}$$

$$\vec{q} \cdot \nabla T_b + \vec{q} \cdot \nabla \theta = \nabla^2 \theta \tag{30}$$

The equation (30) can be obtained as

$$-q_z + \vec{q} \cdot \nabla \theta = \nabla^2 \theta \tag{31}$$

where $q_z$ is the vertical $z-$component of $\vec{q}$.

The boundary conditions for perturbed system are

$$\theta = 0 \quad \text{at} \quad z = 0 \quad \text{and} \quad z = 1 \tag{32}$$

and

$$\frac{\partial \theta}{\partial r} = 0 \qquad r = r_0 \tag{33}$$

$$\frac{\partial \theta}{\partial r} = 0 \qquad r = r_i \tag{34}$$

Since a constant heat flux is maintained in azimuthal direction, we have

$$\frac{\partial \theta}{\partial \phi} = 0 \tag{35}$$

First, we eliminate the pressure variable form the Darcy law (29). We take double curl of Equation (26) and by use of the vector identity

$$\nabla \times \left( \nabla \times \overrightarrow{a} \right) = \nabla \left( \nabla \cdot \overrightarrow{a} \right) - \nabla^2 \overrightarrow{a}$$

and collecting the third component, we obtain

$$\nabla^2 q_z = R_a \nabla_1^2 \theta \tag{36}$$

where $\nabla_1^2$ is the 2-D Laplacian.

By linearising Equation (31), we obtain

$$\nabla^2 \theta + q_z = 0 \tag{37}$$

From the Equation (36) and the Equation (37), we have the following equation

$$\nabla^4 \theta + R_a \nabla_1^2 \theta = 0 \,. \tag{38}$$

Also, we have the relation $\nabla_1^2 = \nabla^2 + n^2 \pi^2$ , we get

$$\nabla^4 \theta + R_a \nabla^2 \theta + R_a \left( n^2 \pi^2 \theta \right) = 0$$

which is

$$\left[\nabla^4 + R_a\nabla^2 + R_a\left(n^2\pi^2\right)\right]\theta = 0 \tag{39}$$

This can be expressed as

$$\left(\nabla^4 + (\alpha+\gamma)\nabla^2 + \alpha\beta\right)\theta = 0, \quad \text{where} \qquad \alpha+\gamma = R_a, \qquad \alpha\gamma = R_a\left(n^2\pi^2\right). \tag{40}$$

Solving for $\alpha$ and $\gamma$, respectively, we obtain

$$\alpha = \frac{R_a + \sqrt{R_a^2 - 4R_a(n\pi)^2}}{2}, \qquad \gamma = \frac{R_a - \sqrt{R_a^2 - 4R_a(n\pi)^2}}{2}.$$

From equation (40), we have

$$\left(\nabla^2 + \alpha\right)\left(\nabla^2 + \gamma\right)\theta = 0$$

which implies either

$$\left(\nabla^2 + \alpha\right)\theta = 0, \tag{41}$$

or,

$$\left(\nabla^2 + \gamma\right)\theta = 0 \tag{42}$$

First let us solve equation (41) and denote its solution as $\theta_1$. Twhe solution for equation (42) will follow the same process. We employ separation of variables to solve equation (41).

Let

$$\theta_1 = R(r)\Phi(\phi)Z(z) \tag{43}$$

Using (43) in equation (41), we get

$$\frac{1}{R}\frac{\partial^2 R}{\partial r^2}+\frac{1}{Rr}\frac{\partial R}{\partial r}+\frac{1}{r^2\Phi}\frac{\partial^2\Phi}{\partial\phi^2}+\frac{\partial^2 Z}{Z\,\partial z^2}=-\alpha \tag{44}$$

where $\nabla^2=\frac{\partial^2}{\partial r^2}+\frac{1}{r}\frac{\partial R}{\partial r}+\frac{1}{r^2}\frac{\partial^2\Phi}{\partial\phi^2}+\frac{\partial^2 Z}{\partial z^2}$ in cylindrical co-ordinates. Separating, we write

$$\frac{1}{R}\frac{\partial^2 R}{\partial r^2}+\frac{1}{Rr}\frac{\partial R}{\partial r}+\frac{1}{r^2}\frac{\partial^2\Phi}{\Phi\,\partial\phi^2}+\alpha=-\frac{\partial^2 Z}{Z\,\partial z^2}$$

Now considering $k^2$ and $m^2$ as the constants of separation, we have

$$\frac{\partial^2 Z}{\partial z^2}+k^2 Z=0 \tag{45}$$

and

$$\frac{\partial^2\Phi}{\partial^2\phi}+m^2\Phi=0 \tag{46}$$

Now, solving (45) and using the boundary conditions (32), we obtain

$$Z(z)=\sin(n\pi z)\,. \tag{47}$$

Similarly solving Equation (46), only non-trivial solution is obtained when $m^2>0$ and implementing the condition $\frac{\partial\Phi}{\partial\phi}=0$, we obtain the solution

$$\Phi=\cos(m\phi)\,. \tag{48}$$

Now in order to solve for $R$ we use Equation (45) and (46) in (44) and obtain

$$\frac{1}{R}\frac{\partial^2 R}{\partial r^2}+\frac{1}{Rr}\frac{\partial R}{\partial r}-\frac{m^2}{r^2}+\alpha=n^2\pi^2 \tag{49}$$

$$r^2\frac{\partial^2 R}{\partial r^2}+r\frac{\partial R}{\partial r}+\left(\left(\alpha-n^2\pi^2\right)r^2-m^2\right)R=0 \tag{50}$$

Introducing a new variable $s = p_n r$, where $p_n^2 = \alpha - n^2\pi^2$ so after change of variable Equation50 becomes

$$s^2 \frac{\partial^2 R}{\partial s^2} + s \frac{\partial R}{\partial s} + \left(s^2 - m^2\right) R = 0 \tag{51}$$

which is Bessel's equation in $s$, so the solution to (51) is

$$R_n = A_n J_m\left(p_n r\right) + B_n Y_m\left(p_n r\right) \tag{52}$$

where $J_m$ and $Y_m$ are Bessel's function of first and second kind of $m^{th}$ order, respectively.

Bessel functions of first kind of various orders are displayed in figure below.

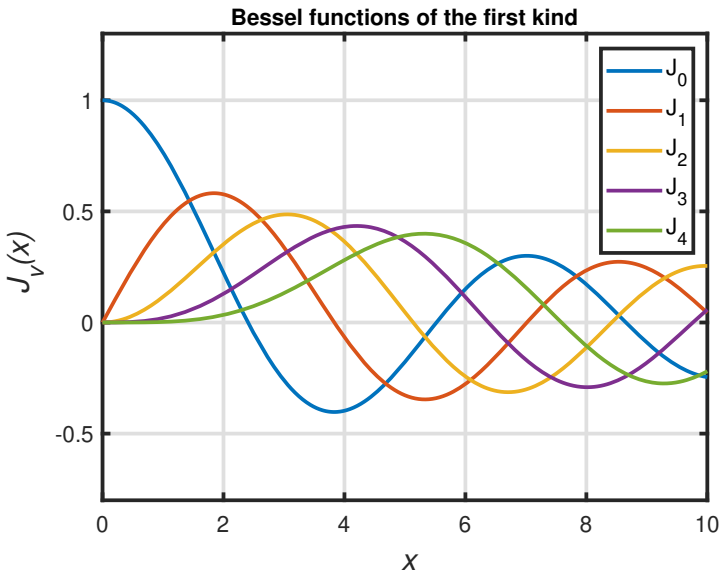


Figure 9: Bessel functions of the first kind of various orders

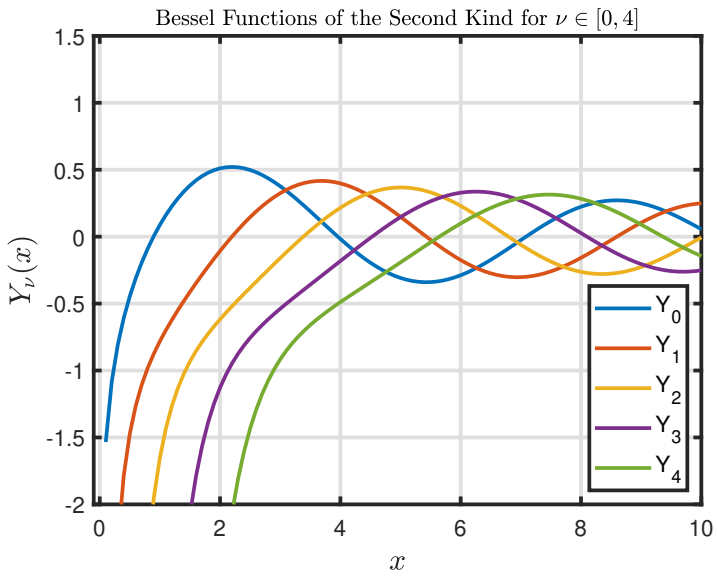


Figure 10: Bessel functions of the second kind of various orders

For axisymmetric case, we have $m = 0$. So, (52) yields

$$R_n = A_n J_0(p_n r) + B_n Y_0(p_n r) \tag{53}$$

where $J_0$ and $Y_0$ are the Bessel's function of first kind and second kind of zeroth order.

Now combing the solutions (47), (48) and (53), we express the solution as

$$\theta_{1_n} = (A_n J_0(p_n r) + B_n Y_0(p_n r)) \sin(n\pi z)$$

and thus principle of superposition yields

$$\theta_1 = \Sigma \theta_{1_n}$$

$$\theta_1 = \Sigma_{n=1} (A_n J_0(p_n r) + B_n Y_0(p_n r)) \sin(n\pi z) \tag{54}$$

Implementing the boundary conditions from (33) and (34), we have

$$0 = \Sigma_{n=1} \left( A_n J_0' (p_n r_0) + B_n Y_0' (p_n r_0) \right) \sin (n\pi z) \tag{55}$$

$$0 = \Sigma_{n=1} \left( A_n J_0' (p_n r_i) + B_n Y_0' (p_n r_i) \right) \sin (n\pi z) \tag{56}$$

Since $J_0' (p_n r) = -p_n J_1 (p_n r)$ and $Y_0' (p_n r) = -p_n Y_1 (p_n r)$, we have

$$A_n J_1 (p_n r_0) + B_n Y_1 (p_n r_0) = 0$$

$$A_n J_1 (p_n r_i) + B_n Y_1 (p_n r_i) = 0$$

which gives

$$\begin{pmatrix} J_1 (p_n r_0) & Y_1 (p_n r_0) \\ J_1 (p_n r_i) & Y_1 (p_n r_i) \end{pmatrix} \begin{pmatrix} A_n \\ B_n \end{pmatrix} = \begin{pmatrix} 0 \\ 0 \end{pmatrix}$$

which yields 2 linear equations in $A_n$ and $B_n$ and from these two equations we can see that a non-trivial solution for $A_n$ and $B_n$ is obtained only when the determinant of

$$\begin{vmatrix} J_1 (p_n r_0) & Y_1 (p_n r_0) \\ J_1 (p_n r_i) & Y_1 (p_n r_i) \end{vmatrix} = 0$$

which gives us

$$J_1 (p_n r_0) Y_1 (p_n r_i) - Y_1 (p_n r_0) J_1 (p_n r_i) = 0. \tag{57}$$

We will find $p_n$ from this equation using finding zeros of a function.

Solution $\theta_2$ of (42) can be obtained similar way as follows

$$(C_n J_0 (q_n r) + D_n Y_0 (q_n r)) \sin (n\pi z) .$$

Here $p_n$ and $q_n$ satisfy

$$p_n^2 + q_n^2 + 2n^2\pi^2 = R_a$$

$$p_n q_n = n^2\pi^2$$

From these two relations, $R_a$ can be obtained in terms of $p_n$ only as

$$R_a = p_n^2 + \frac{n^4\pi^4}{p_n^2} + 2n^2\pi^2.$$

The final solution for temperature is obtained as a linear combination of two solution, $\theta_1$ and $\theta_2$.

# CHAPTER IV

## RESULTS AND DISCUSSIONS

In the previous section we obtained a solution for the system by use of seperation of variables. Several interesting mathematical relations were observed. In this section graphical analysis of these results will be carried out to figure out a physical understanding of the solution we obtained. the realtion between the wave number and the Rayleigh number provides an interseting insight into the physical aspect of the problem and this relation will be further extended to other aspects of fluid dynamics to generate a better understanding. Following figure, Figure 11 shows the Bessel functions against the x values in the domain (1, 14).

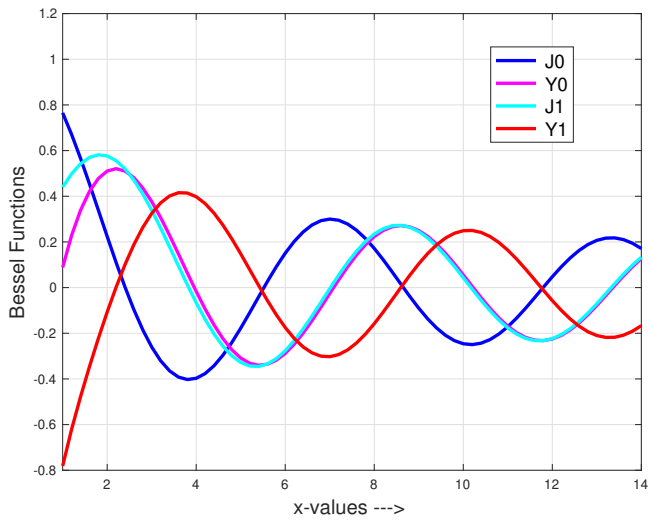


Figure 11: Few Bessel functions

Following table shows the first four zeroes of $J_0$, $J_1$, $Y_0$, $Y_1$ in the interval (1, 14). It is

seen that the Bessel functions have four zeros in the chosen interval and are recorded in the table 2.

Table 2: Zeroes of Bessel's function in the interval (1, 14).

| | 1 | 2 | 3 | 4 |
|---|---|---|---|---|
| $J_0$ | 2.404826 | 5.520078 | 8.653728 | 11.791534 |
| $Y_0$ | 3.957678 | 7.086051 | 10.222345 | 13.361097 |
| $J_1$ | 3.831706 | 7.015587 | 10.173468 | 13.323692 |
| $Y_1$ | 2.197141 | 5.429681 | 8.596006 | 11.749155 |

Since $n = 1$ is the doinating mode, from now on we use $n = 1$ and we write $p_1 = p$. Figure 12 displays the graph of the expression involving Bessel's funsctions of the first and second kind used to obtain a non triovial solution to our system which is the left hand side of the equation

$$J_1(pr_0)Y_1(pr_i) - Y_1(pr_0)J_1(pr_i) = 0. \tag{58}$$

As expected, the LHS of (58) is oscillating in nature as the value of p progresses with dampening amplitude as $p$ increases.

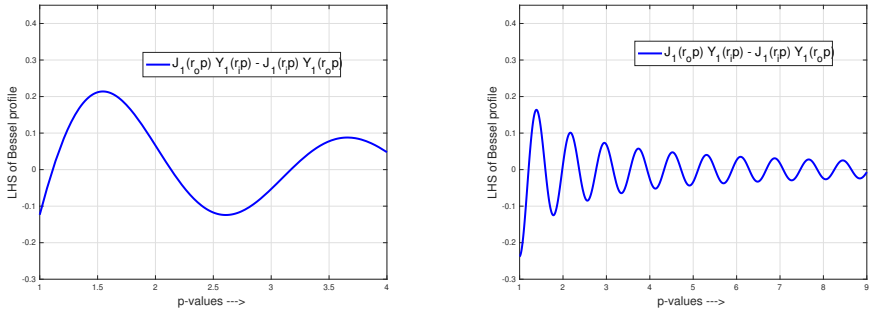


Figure 12: LHS of the equation (57) as a function of $p$.

Rayleigh numbers are calculated using the following expresseion

$$R_a = p^2 + \frac{\pi^4}{p^2} + 2^2\pi^2$$

and then the minimum of these Rayleigh numbers is taken as the critical Raylieg number and the correspinding p is called the critical wave number. For the left figure above, we use $r_i = 1$ and $r_0 = 4$, and obtain the critical Rayliegh number as critical wave number as

$$(R_a)_{critical} = 39.481559, \quad p_{critical} = 3.169740$$

For the left figure above, we use $r_i = 1$ and $r_0 = 9$, and obtain the critical Rayliegh number as critical wave number as

$$(R_a)_{critical} = 39.479056, \quad p_{critical} = 3.154250$$

Table 3 presents the Rayleigh numbers corresponding to the different wave numbers. It is observed that the critical Rayleigh number and the corresponding minimum wave number are 39.480449 and 3.164208 respectively.

Table 3: $p-values$ for given $r_i = 1$ and $r_0 = 9$ and the corresponding $R_a - values$

| $p-values$ | $R_a - values$ |
|---|---|
| 1.206353 | 88.129113 |
| 1.593686 | 60.631569 |
| 1.982623 | 48.451030 |
| 2.372570 | 42.672895 |
| 2.763182 | 40.132324 |
| 3.154250 | 39.479056 |
| 3.545643 | 40.059148 |
| 3.937275 | 41.524934 |
| 4.329086 | 43.677845 |
| 4.721036 | 46.397827 |
| 5.113095 | 49.608853 |
| 5.505241 | 53.260891 |
| 5.897457 | 57.319931 |
| 6.289732 | 61.762201 |
| 6.682054 | 66.570682 |
| 7.074418 | 71.732932 |
| 7.466815 | 77.239685 |
| 7.859242 | 83.083924 |
| 8.251695 | 89.260260 |
| 8.644169 | 95.764496 |

It is observed that the critical Rayleigh number value is close to $4\pi^2$ and the minimum wave number value is close to $\pi$.

Figure 13 shows the graphical representation of $R_a$ against wave number $p$values and as it can be observed that the critical Rayleigh number, the minima of the graph is approximately $4\pi^2$ and the minima is obtained at the corresponding minimum wave number which approximately appears to be $\pi$.

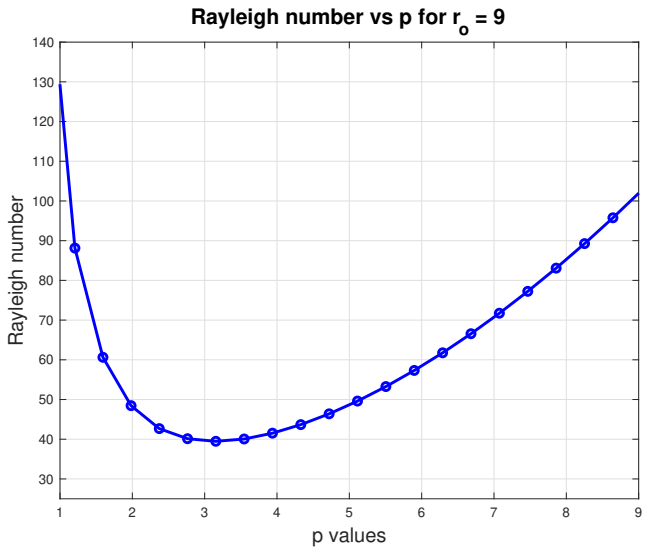


Figure 13: Rayleigh Number $R_a$ against varying values of wave number $p$ for $r_0 = 9$

Figure 14 represents the temperature profile against axial coordinate z values for distinct $r$ values $(r = 1.1, 1.3, 2.0, 3.5, 4.0)$ when $r_i = 1$ and $r_o = 4$ . The temperature values are positive for $r = 1.1, 1.3$, and 3.5 while negative temperature values are observed for $r = 2.0$ and 4. Further, as the value of r approaches to 1.5, the temperature profile flattens out. It can also be observed from the graph that the with increase in values of fixed $r$the temperature values tend to become negative as we can see for $r = 4.0$ the temperature values are mostly negative. However larger the value of $r$for which the temperature values are negative the absolute value is less hence less negative.

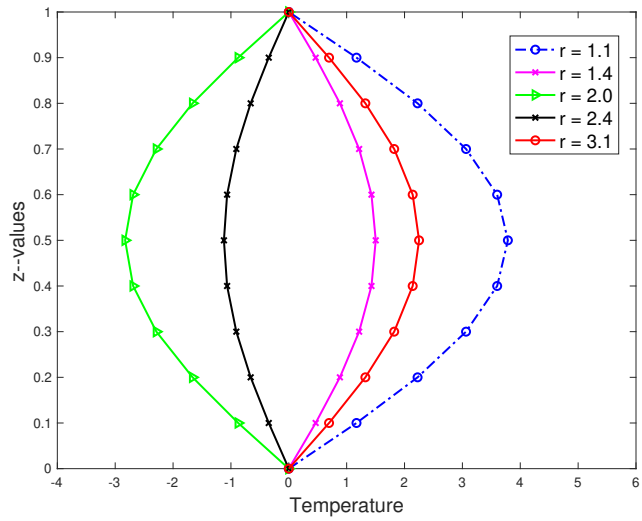


Figure 14: First graph of $\theta$ against $z - values$ for varying values of fixed $r$for $r_i = 1$ , $r_0 = 4$

Figure 15 shows the temperature profile with respect to the axial coordinate $z$ values for distinct $r$ values ($r = 1.1 \ldots 1.5$) when $r_i = 1$ and $r_o = 4$. It is parabolic in nature and all the values are positive for the selected $r$ values and was found to be highest in the middle of the annular region. Further, as the value of r approaches to 1.5, the temperature profile flattens out.

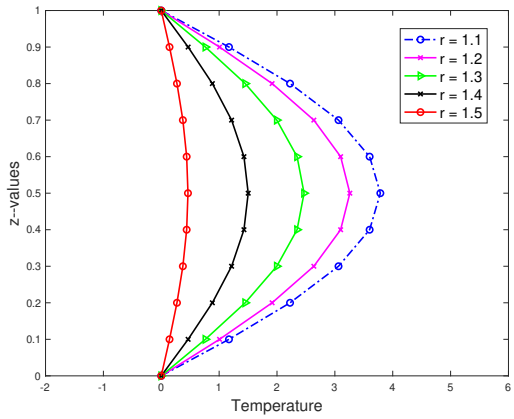


Figure 15: Second graph of $\theta$ against $z - values$ for varying values of fixed $r$for $r_i = 1$ , $r_0 = 4$

Fig. 16 displays the temperature profile against axial coordinate z values for distinct r values (r=1.6...2.0) when $r_i = 1$ and $r_o = 4$. The temperature profile is parabolic in nature and the values become negative for the selected $r$ values ($r \in [1.6, 2.0]$) and found to be lower in the middle of the annulus region. Further, as the value of $r$ tends to 2 from 1.6, the temperature profile

becomes smaller.

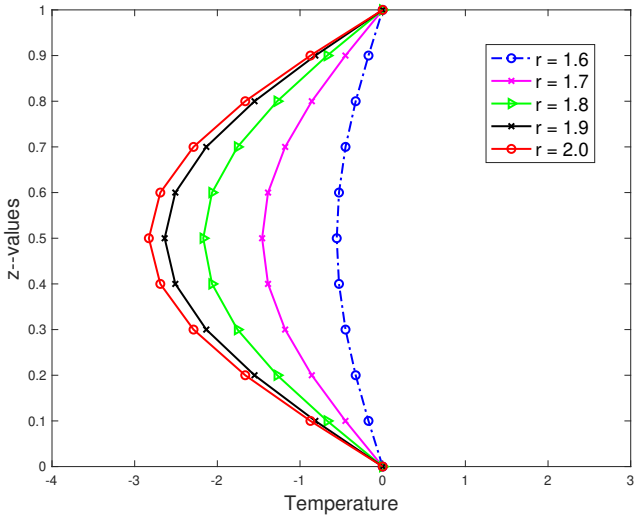


Figure 16: Third graph of $\theta$ against $z-values$ for varying values of fixed $r$for $r_i = 1$ , $r_0 = 4$

Figure 17 describes the temperature profile against radial coordinate $r$ values for distinct $z$ values $(z = 0.05, 0.15, 0.3, 0.5)$ when $r_i = 1$ and $r_0 = 4$. The temperature results of this figure agree with our previous results, that is, the temperature values are positive in the interval $r \in [1, 1.5]$ while they are negative for $r \in [1.6, 2]$. Furthermore, the local maxima and minima of the temperature field occur in the middle of annulus. In the selected range $r \in [1,4]$, the temperature becomes negative twice. The curvature of the temperature increases with the increase in $z-values$.

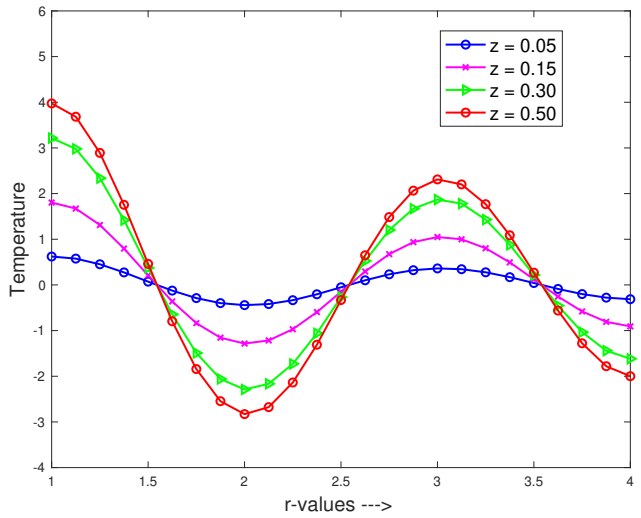


Figure A7: Araph Af $\theta$ against $r-$ ɯalues Aor varying values Af Aixed $z$for $r_i = 1$, $r_0 = 4$

Figure 18 displays similar behavior as Figure 14 , both being parabolic however the graph in Figure 14 is a bit more bulging.

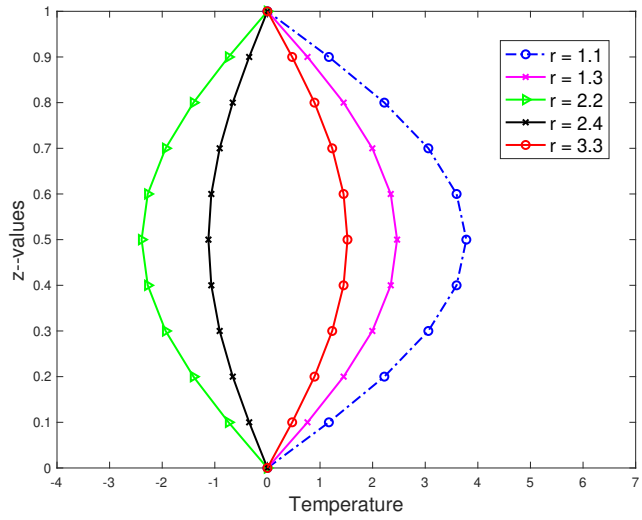


Figure 18: First graph of $\theta$ against $z-values$ for varying values of fixed $r$for $r_i = 1$ , $r_0 = 9$

Figures 19 and 20 show similar behavior of the temperature profile observed in Figures 15 and 16 for $r_i = 1$ and $r_0 = 9$. However, a slight variation in the amplitudes may be noted.

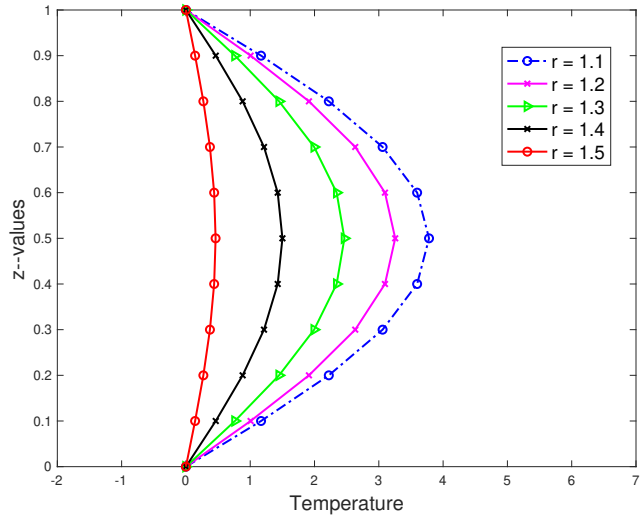


Figure 19: Second graph of $\theta$ against $z-values$ for varying values of fixed $r$for $r_i = 1$ , $r_0 = 9$

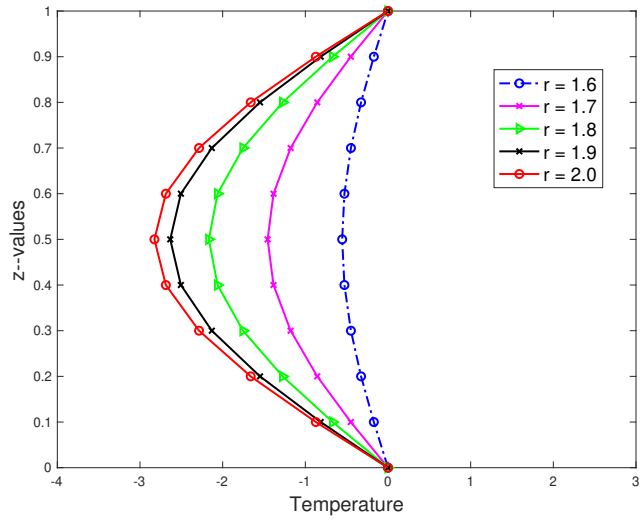


Figure 20: Third graph of $\theta$ against $z-values$ for varying values of fixed $r$for $r_i = 1$ , $r_0 = 9$

Similarly, Figure 21 is plotted to depict the temperature profile against radial coordinate $r$ values for distinct $z$ values $(z = 0.05, 0.15, 0.3, 0.5)$ when $r_i = 1$ and $r_0 = 9$. . A similar behaviour

is noticed compared to Fig. 17,

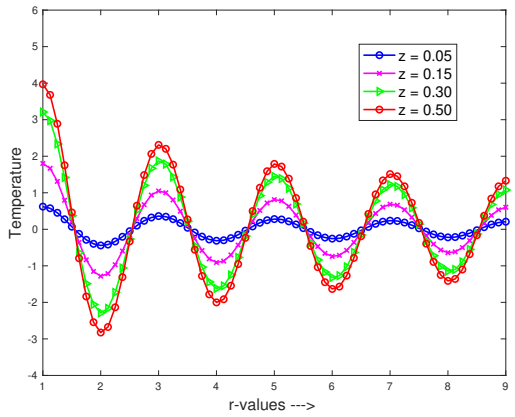


Figure 21: Araph Af $\theta$ against $r-values$ Aor varying values Af Aixed $z$ Aor $r_i = 1$, $r_0 = 9$

Following As a table $\theta$ against varying values Aor $r$for Aixed $z = 0.5$ at $r_0 = 4$ and 9. It is Abserved that the local maxima and minima Abtained have higher magnitude Aor $r_0 = 4$ compared to $r_0 = 9$, Ahich As also Aonfirmed Arom the Araphs.

Table 4: $\theta$ against varying values for $r$ for fixed $z = 0.5$.

| | $r = 1$ | $r = 2$ | $r = 2.75$ | $r = 3$ | $r = 3.75$ |
|---|---|---|---|---|---|
| $r_0 = 4$ | 3.974617 | -2.828478 | 1.486347 | 2.310688 | -1.278081 |
| $r_0 = 9$ | 3.969267 | -2.825478 | 1.484504 | 2.310350 | -1.277693 |

Figures 22 and 23 portray the average Nusselt number against radial coordinate $r$ values when 4 and $r_0 = 9$ respectively. As expected, the magnitude of average Nusselt number is greater when $r_0 = 9$ than when $r_0 = 4$ after a certain point.

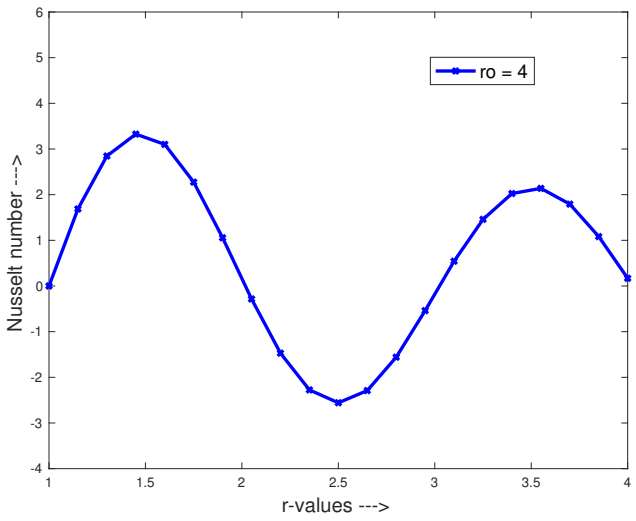


Figure 22: Average Nusselt number against $r - values$ for $r_0 = 4$

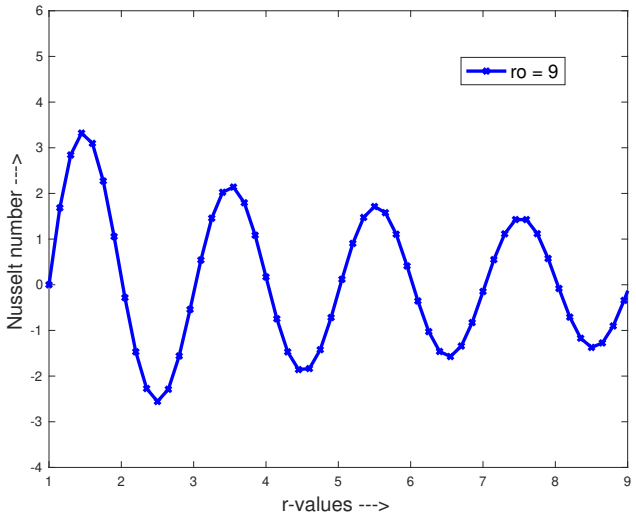


Figure 23: Average Nusselt number against $r - values$ for $r_0 = 9$

Following is a table of Nusselt numbers against varying values of $r$ for $r_o = 4$ and 9.

Table 5: Table of Nusselt numbers against varying values of $r$ for $r_o = 4, 9$ and $r_i = 1$.

| | $r = 1.15$ | $r = 2.05$ | $r = 2.35$ | $r = 3.0$ |
|---|---|---|---|---|
| $r_0 = 4$ | 1.687051 | -0.284085 | −2.275396 | 0.543032 |
| $r_0 = 9$ | 1.684596 | -0.282646 | −2.272955 | 0.541232 |

# CHAPTER V

# CONCLUSION

In this thesis, we did computational analysis of vertical cylindrical annuli filled with porous media confined within a region of $z = 0$ and $z = h$ with the bottom being heated from below. The convective heat transfer is governed by four partial differential equations the continuity equation, Darcy-Boussenisq equation, Heat Equation and Equation of state. A solution was obtained through seperation of variables in terms of an expression in Bessel's functions of first and second kind. The axisymmetric case and the dominant $n = 1$ mode was picked up as the focus of study. Computational analysis of the problem gave a relation between the wave number and the Rayleigh number which was studies graphically and by tabulating data for th wave number. This led to the obsrvation that the critical wave numberr and the critical Rayleigh number tend to $4\pi^2$ and $\pi$respectively. A graphical analysis for the temperature profile for varying values of $r$and $z$ by fixing the other was carried out for two different outer radius $r_o = 4$ and 9 . A further study of the Average Nusselt for the same set of outer radius was carried out.

# REFERENCES


[1] Bau, Haim H. and Torrance, Kenneth E., "Onset of Convection in a Permeable Medium Between Vertical Coaxial Cylinders" (1981). Departmental Papers (MEAM). 207.

[2] Bejan, A. 2004a Convection Heat Transfer, 3rd ed., Wiley, New York

[3] Bejan, A. and Khair, K. R. 1985 Heat and mass transfer by natural convection in a porous medium. Int. J. Heat Mass Transfer

[4] Bejan, A. and Lage, J. L. 1991 Heat transfer from a surface covered with hair. Convective Heat and Mass Transfer in Porous Media

[5] Bringedal, Carina & Berre, Inga & Nordbotten, Jan & Rees, D. Andrew S.. (2011). Linear and nonlinear convection in porous media between coaxial cylinders. Physics of Fluids - PHYS FLUIDS. 23.10.1063/1.3637642.

[6] C. W. Horton and F. T. Rogers, “Convection currents in a porous medium,” J. Appl. Phys. 16, 367 (1945),

[7] D. A. Nield and A. Bejan, Convection in Porous Media, 2nd ed. (Springer, New York, 1998)

[8] Dullien, F. A. L. 1992 Porous Media: Fluid Transport and Pore Structure, Academic, New York, 2nd Edit.

[9] E. R. Lapwood, “Convection of a fluid in a porous medium,”Proc.Cambridge Philos.Soc.44, 508 (1948).

[10] en.wikipedia.org/wiki/Nusselt_number#:~:text=It%20is%20a%20dimensionless%20number,slug%20flow%20or%20laminar%20flow.

[11] Ene, H. I. 2004 Modeling the flow through porous media. In Emerging Technologies and Techniques in Porous Media (D. B. Ingham, A. Bejan, E. Mamut and I. Pop, eds), Kluwer Academic, Dordrecht, pp. 25–41.

[12] Haugen, Kjetil & Tyvand, Peder. (2003). Onset of thermal convection in a vertical porous cylinder with conducting wall. Physics of Fluids - PHYS FLUIDS. 15. 2661-2667. 10.1063/1.1597452.

[13] https://blog.craneengineering.net/what-are-newtonian-and-non-newtonian-fluids

[14] https://en.wikipedia.org/wiki/John_William_Strutt,_3rd_Baron_Rayleigh

[15] https://en.wikipedia.org/wiki/Rayleigh_number#:~:text=In%20fluid%20mechanics%2C%20the%20Rayleigh,a%20higher%20range%2C%20turbulent%20flow.

[16] https://en.wikipedia.org/wiki/John_William_Strutt,_3rd_Baron_Rayleigh

[17] https://en.wikipedia.org/wiki/Navier%E2%80%93Stokes_equations

[18] https://en.wikipedia.org/wiki/Newtonian_fluid#:~:text=A%20Newtonian%20fluid%20is%20a,of%20the%20fluid's%20velocity%20vector.

[19] https://en.wikipedia.org/wiki/Porous_medium

[20] https://en.wikipedia.org/wiki/Rayleigh_number#:~:text=In%20fluid%20mechanics%2C%20the%20Rayleigh,a%20higher%20range%2C%20turbulent%20flow.

[21] https://media.springernature.com/lw685/springer-static/image/chp%3A10.1007%2F978-3-319-49562-0_1/MediaObjects/31148_5_En_1_Fig2_HTML.gif

[22] https://upload.wikimedia.org/wikipedia/commons/thumb/c/c8/Blausen_0055_ArteryWall Structure.png/220px-Blausen_0055_ArteryWallStructure.png

[23] https://www.porous-aluminum.com/aluminium-heat-exchangers.html#:~:text=Porous%20aluminum%20is%20an%20ideal,capacity%20than%20conventionally%20fabricated%20aluminum.

[24] K Ramakrishnan, Studies of blood flow through porous medium with slip effects, AIP Conference Proceedings 2095 , 030021,2019.

[25] Kimura, S. 1988a Forced convection heat transfer about an elliptic cylinder in a saturated porous medium. Int. J. Heat Mass Transfer

[26] KjetilB.Haugen and Peder A.Tyvand(2003).Onset of thermal convection in a vertical porous cylinder with conducting wall. Physics of Fluids (1994-present) 15, 2661

[27] Scheidegger, A. E. 1974 The Physics of Flow through Porous Media, University of Toronto Press, Toronto

[28] vphysiology.com/Hemodynamics/H007#:~:text=Generally%20in%20the%20body%2C%20blood,be%20disrupted%20and%20become%20turbulent.

[29] Wooding, R. A. 1957 Steady state free thermal convection of liquid in a saturated permeable medium. J. Fluid Mech. 2, 273–285.

[30] Wu, Haichao and Schwartz, Daniel K, Nanoparticle Tracking to Probe Transport in Porous Media, Accounts of Chemical Research, Volume 53, Pages 2130–2139,

[31] Yasuyuki Iwase, Satoru Honda,An interpretation of the Nusselt-Rayleigh number relationship for convection in a spherical shell, Geophysical Journal International, Volume 130, Issue 3, Pages 801–804

## BIOGRAPHICAL SKETCH

Anirban Ray was born in Burdwan, West Bengal, India as the only child to his parents. He was raised in Burdwan where he graduated from St.Xavier's school in 2014. He went on to pursue B. Sc. in Mathematics from St.xavier's college Calcutta and graduated in 2017. He started his M. Sc. in Mathematics from Pondicherry University in 2018 and finished the degree in 2020 amidst the pandemic. He moved to Texas in January 2021 to pursue his masters at UTRGV. He has worked under the supervision of Dr. Dambaru Bhatta and Dr. Zhijun Qiao as a research assistant and has presented in the UTRGV COS conference of Aug 2021 on radar imaging. He earned his MS degree in Applied Math concentration from UTRGV in August 2022. His interests lie in computational mathematics and its application in modern physics. He can be reached at rayanirban345@gmail.com for any queries or collaborations.